Siglec-E negatively regulates the activation of Toll-like Receptor 4 by controlling its endocytosis

Yin Wu, **Dongren Ren**, and **Guo-Yun Chen**[*]
Children's Foundation Research Institute, Department of Pediatrics, University of Tennessee Health Science Center, Memphis, TN 38103

Abstract

TLR4 signaling is critical for providing effective immune protection but must be tightly controlled to avoid inflammation-induced pathology. Previously, we reported extensive and direct interactions between Toll-like receptor and Siglec families of Pattern Recognition Receptors. Here, we examined the biological significance of this interaction during infection. We show that Siglec-E is required for *E. coli*-induced endocytosis of TLR4. Siglec-E-deficient dendritic cells infected with *E. coli* fail to internalize TLR4, leading to sustained TLR4 on cell surface and activation of NF-κB and MAP kinase p38, thus resulting in high levels of TNF-α and IL-6, compared with wild-type dendritic cells. In contrast to the signaling events occurring at the plasma membrane, as a result of the inability of internalization of TLR4, Siglec-E-deficient dendritic cells were also defective for TRIF-mediated IFN-β production in response to *E. coli* infection. Furthermore, we found that accumulation of ubiquitinated-TLR4 and binding of E3 ubiquitin ligase Triad3A to TLR4 was significantly increased in bone marrow-derived dendritic cells from wild-type mice but not from Siglec-E-deficient mice after *E. coli* infection. This represents a newly discovered mechanism that regulates the signaling of TLR4 during *E. coli* infection.

Introduction

Sepsis is one of the leading causes of death in intensive care units. Of the more than 1 million Americans who are diagnosed with severe sepsis every year, between 28 and 50 percent die from this disease (1, 2). The majority of cases of septic shock are caused by Gram-negative bacteria, and *E. coli* remains one of the most common pathogens leading to sepsis (3–5). Because of the critical role of cytokine storms in the development of septic shock (6, 7), inflammatory cytokines and other inflammatory mediators such as nitric oxide have been targeted for therapeutic development. However, phase III clinical trials of nitric oxide synthase inhibition (8) and immunotherapies targeting individual cytokines (9) have limited effect on sepsis progression, and the identification of additional druggable targets are urgently needed to effectively treat this disease.

Sialylation is the most frequent modification of proteins and lipids, and describes the addition of sialic acids (a family of nine-carbon acidic monosaccharides) to terminal

[*]To Whom correspondence should be addressed: Children's Foundation Research Institute, Department of Pediatrics, University of Tennessee Health Science Center, Memphis, TN, 38103. Tel: 901-287-6883; Fax: 901-287-4551; Gchen14@uthsc.edu.

residues of glycoproteins and glycolipids. Sialylation plays an important role in self-nonself discrimination and bacterial intake (10, 11). Increases of sialylation contribute to the tolerant phenotype in CD4^{+} T cells (12), dendritic cells, macrophages (13) and regulatory T cells (14); while desialylation acts as an "eat me" signal and promotes the clearance of apoptotic cells (15). The sialylation level of a cell is largely dependent on the activity of two enzymes; sialyltransferases, which are responsible for adding sialic acid residues to glycolipids or glycoproteins; and sialidases, which are responsible for removing sialic acid residues from glycolipids or glycoproteins.

Siglecs are membrane-bound lectins that constitute the sialic acid-binding immunoglobulin-like super family, each with distinct cellular distribution and glycan specificities (16). Siglecs predominantly bind to sialic acids on cell surface proteins (17), and play an important role in the internalization of sialic acid-expressing pathogens (18–20), in controlling allergic asthma (21, 22), and in self-tolerance (23). Previously, we found that interaction between CD24 and SiglecG/10 is a key regulator of polybacterial sepsis, and this interaction requires sialylation of CD24 (24, 25). We recently reported extensive and direct interactions between Siglecs and Toll-like receptors (TLRs), and demonstrated that dendritic cells from Siglec-E-deficient mice exhibit increased responses to all TLR ligands tested (26), however, the biological significance of the novel pathway in sepsis development is still unknown.

The endocytosis of immunity-related receptors has emerged as a critical control step in the signal transduction process. While it has been reported that the endocytosis of plasma membrane-localized TLRs downregulates their signaling functions after a microbial encounter (27, 28), little is known about the regulators that control TLR endocytosis after microbial detection. Recent studies suggested that endocytic activity is a general property of the Siglec family proteins (20, 29–32), with Siglecs identified as key players in both the binding and uptake of sialylated pathogens (20, 33–36) and in the endocytosis of anti-CD22 antibody (37), however, it is unknown whether Siglecs play a role in mediating endocytosis of membrane receptors during infection.

In the present study, we found that cell surface desialylation of innate immune cells inhibits the endocytosis of TLR4 on these cells during *E. coli* infection. Furthermore, we report here that Siglec-E is required for endocytosis of TLR4, and this Siglec-E mediated endocytosis is partially due to the action of protein kinases Src, GSK and ERK. Our findings describe a newly discovered mechanism that regulates the signaling of TLR4 during *E. coli* infection.

Material and Methods

Reagents

Anti-mouse TLR4 (MTS510), TLR2, CD64 and Gr-1 antibodies were purchased from Biolegend (San Diego, CA). Anti-Siglec-E was obtained from R&D system (Minneapolis, MN). Anti-mouse CD11c, CD11b and B220 were purchased from BD Biosciences (San Jose, CA). Anti-TRIAD3A (catalog no. PA5-20079) was obtained from ThermoFisher Scientific (Waltham, MA). Anti-Flag was purchased from Sigma (St Louis, MO). Anti-P-Src (catalog no. 2109), Anti-AKT (catalog no.4060), Anti-P-S6 (catalog no. 2708), Anti-PKC α

(catalog no. 2056) and Phospho-PKCα/β II (Thr638/641) Antibodies (catalog no. 9375) were obtained from Cell Signaling (Danvers, MA). P65 (catalog no. sc-109), P-P65 (catalog no. sc-33020), JNK (catalog no. sc-7345), P-JNK (catalog no. sc-6254), ERK (catalog no. sc-94), P-ERK (catalog no. sc-7383), β-actin (catalog no. sc-1615), p38 (catalog no. sc-535), p-p38 (catalog no. sc-17852), Sp-1 (catalog no. sc-59), IRF3 (catalog no. sc-9082), antibodies, and horseradish perioxidase conjugated anti-mouse, anti-goat or anti-rabbit secondary-step reagents were purchased from Santa Cruz Biotechnology (Dallas, TX). Syk inhibitor piceatannol, Src inhibitor PP1, PD98059 (MEK inhibitor), SP600125 (JNK inhibitor), SB203580 (P38 inhibitor), Wortmannin (PI3K inhibitor), GÖ6976 (PKC inhibitor), GSK inhibitor (SB216763), ERK inhibitor were purchased from Santa Cruz Biotechnology. Biotinylated Maackia Amurensis Lectin II (MAL II) (catalog no. B-1265) and Biotinylated Sambucus Nigra Lectin (SNA, EBL) (catalog no. B-1305) were purchased from Vector Laboratories (Burlingame, CA). NEURAMINIDASE (SIALIDASE) from Vibrio cholerae (catalog no. 11080725001) was purchased from Sigma.

Cell culture and lentiviral infection

D2SC/1 dendritic cells were obtained from Dr. Peter G. Stock and Sang-Mo Kang (University of California, San Francisco, CA) with the permission from Dr. Paola Ricciardi-Castagnoli (University of Perugia, Italy), and maintained in Dulbeco's minimal essential medium supplemented with 10% heat-inactivated fetal calf serum and 1% penicillin and streptomycin. The lentiviral vectors expressing either Neu1, Siglec-e or Siglec-g shRNAs were from ThermoFisher Scientific. Puromycin was purchased from Sigma. Stable clones were obtained after selection with puromycin (2.5 μg/ml) for 2 weeks after infection.

Experimental animal models

All mice used were at 6–8 weeks of age, and wild-type (WT) littermates were used as controls for Siglec-E knockout mice. All animal procedures were approved by the Animal Care and Use Committee of University of Tennessee Health Science Center. WT C57BL/6J mice were purchased from Jackson Laboratory. CD14 knockout mice were obtained from Jackson Laboratory. Siglec-E knockout mice were from Mutant Mouse Regional Resource Center at UC Davis. The mice were backcrossed to C57BL/6J background.

Construction of plasmids

To generate a construct expressing mouse Neu1, cDNA for Neu1 was amplified by RT-PCR and subcloned into expression vector pcDNA6 (Life technologies). All constructs were verified by restriction enzyme digestion and DNA sequencing. Construct MR206325 expressing mouse ST6Gal1 was obtained from Origene (Rockville, MD).

Bacterial culture

E.coli 25922 was obtained from ATCC (25922). Strains were grown overnight in the Luria-Bertani (LB) broth. In the logarithmic phase of the growth, the suspension was centrifuged at 1000×g for 15 min, the supernatant was discarded, and the bacteria were resuspended and diluted into sterile 1×PBS. *E. coli* GFP was obtained from ATCC (25922GFP) and propagated according to the method provided by the manufacturer.

Preparation of Dendritic Cells from murine bone marrow

Bone marrow cells were isolated from femurs and incubated in RPMI complete medium supplemented with 10% fetal calf serum (Gibco-BRL) and 10 ng/ml recombinant mouse GM-CSF (Peprotech) and 1 ng/ml IL-4 (Peprotech) for 12 days.

Flow cytometry

Spleen cells from WT or Siglec-E knockout mice treated with PBS, *E.coli* 25922 or *E.coli* 25922GFP, or cultured cells were washed with Flow cytometry staining buffer (1×PBS, 2% BSA), and then incubated for 1 hour on ice with different directly conjugated-antibodies. The fluorescence intensity of cells was analyzed on LSRFortess Flow cytometer or Guava easyCyte™ System (EMD Millipore, Merck KGaA, Darmstadt, Germany).

Real-Time Quantitative PCR

Total RNA was extracted with TRIzol (Invitrogen) according to the manufacturer's protocol and reverse transcribed with random primers and Superscript III (Life Technologies). The mRNA expression of TNF-α, IL-6, IFN-β, IFN-γ, Viperin and MCP-1 was measured by real-time polymerase chain reaction. Samples were run in triplicate, and the relative expression was determined by normalizing expression of each target to the endogenous reference, hypoxanthine phosphoribosyltransferase (Hprt) transcripts. Real-time PCR primers used were as follows: TNF-α sense, CTGTAGCCCACGTCGTAGC; TNF-α antisense, TTGAGATCCATGCCGTTG; IL-6 sense, CTCTGGGAAATCGTGGAAAT; IL-6 antisense, CCAGTTTGGTAGCATCCATC; IFN-β sense, TTCCTGCTGTGCTTCTCCAC; IFN-β antisense, AAGGTACCTTTGCACCCTCC; IFN-γ sense, CAATAGACGCTACACACTGC; IFN-γ antisense, CCACATCTATGCCACTTGAG; Viperin sense, CTTCAACGTGGACGAAGACA, Viperin antisense, GACGCTCCAAGAATGTTTCA; MCP-1 sense, TGATCCCAATGAGTAGGCTGGAG, MCP-1 antisense, ATGTCTGGACCCATTCCTTCTTG; Hprt sense, AGCCTAAGATGAGCGCAAGT; Hprt antisense, TTACTAGGCAGATGGCCACA.

Immunoprecipitation and immunoblotting

D2SC/1 cell lysates were prepared in lysis buffer (20 mM Tris-HCl, 150 mM NaCl, 1 % Triton X-100, pH 7.6, with protease inhibitors 1 μg/ml leupeptin, 1 μg/ml aprotinin and 1 mM phenylmethylsulfonyl fluoride). Samples were sonicated, centrifuged at 13,000 rpm for 5 min and diluted in immunoprecipitation (IP) buffer (20 mM Tris-HCl, 150 mM NaCl, pH 7.6, supplemented with the protease inhibitors as described above) and pre-cleared with 60 μl of protein A-conjugated agarose beads (Upstate, Lake Placid, NY) for 1 h at 4°C, before incubation with corresponding antibodies. Immunoprecipitates were washed four times with IP buffer and re-suspended in SDS sample buffer for Western blot analysis.

Measurement of inflammatory cytokines

Blood or cell culture supernatants were obtained at indicated times, and cytokines in the serum or cell culture supernatants were determined using mouse cytokine bead array designed for inflammatory cytokines (BD Biosciences, 552364).

IFN measurement

IFN-β in the cell culture supernatants or serum was determined by using the LEGEND MAX Mouse IFN-β Pre-coated ELISA kit according to manufacturer's instructions (Biolegend, San Diego, CA).

Statistical analysis

The differences in cytokine concentrations were analyzed by two-tail *t*-tests in single pairwise comparisons, calculated with Excel (Microsoft). One-way ANOVA was used for three or more unpaired groups (GraphPad Software). Data shown are mean ± SEM. The differences in survival rates were analyzed by Kaplan-Meier plot and statistical significance determined using a log -rank test (GraphPad Software). *$P<0.05$, **$P<0.01$, ***$P<0.001$, n.s., not significant.

Results

The role of sialylation in *E. coli*-induced TLR4 endocytosis

We recently reported broad and direct interactions between TLR and Siglec families of Pattern Recognition Receptors (PRRs), and that endogenous Siglec-E negatively regulates production of inflammatory cytokines in response to TLR ligands (26). However, the biological significance of this interaction in sepsis development has not yet been established. Since the interaction between TLR and Siglec depends on the sialylation of the TLR4 (26), we first tested whether sialylation on the cell surface contributes to the regulation of *E. coli*-induced TLR4 endocytosis. Splenic cells from WT C57BL/6J mice were treated with sialidase and incubated with *E. coli 25922* at 37°C for one hour and then measured cell surface TLR4 on these splenic cells by a highly sensitive flow cytometry assay. The loss of cell surface expression was used as a readout for TLR4 endocytosis, as previously reported (38, 39). As shown in the Figure 1A, CD11c^{+} splenic cells are resistant to *E. coli*-induced TLR4 endocytosis after sialidase treatment. Flow cytometric intracellular staining showed increasing intracellular TLR4 following *E. coli* infection in cells pretreated with PBS but not in cells pretreated with sialidase (Fig. 1B), indicating sialylation on cell surface plays an important role in the regulation of TLR4 endocytosis in response to *E. coli* infection. The decrease of cell surface sialylation after sialidase treatment was confirmed by flow cytometric analysis (Fig. 1C). Splenic cells treated with sialidase secreted significantly higher levels of TNF-α than the PBS treated controls (Fig. 1D), indicating that sialidase treatment of splenic cells increased their response to *E. coli* infection. In addition to mouse splenic cells, we found that dendritic cell line D2SC/1 cells are also resistant to *E. coli*-induced endocytosis after sialidase treatment (Fig. 1E). Flow cytometric intracellular staining showed increased intracellular TLR4 following *E. coli* infection in D2SC/1 cells pretreated with PBS, but not in cells pretreated with sialidase (Fig. 1F). The decrease of cell surface sialylation after sialidase treatment was confirmed by flow cytometric analysis (Fig. 1G). As shown in Figure 1H, the secretion of TNF-α was significantly increased in response to *E. coli* treatment in cells pretreated with sialidase compared with the cells pretreated with PBS. Taken together, these data suggest that sialylation of cell surface plays an important role in the regulation of TLR4 endocytosis during *E. coli* infection.

The role of Neu1 in *E. coli*-induced TLR4 endocytosis

Sialyltransferases and sialidases are enzymes which are largely responsible for adding or removing sialic acid residues, respectively, on glycolipids and glycoproteins. Mammals have four sialidases, Neu1-4 (40). We have demonstrated that Neu1 plays a critical role in regulating Siglec-TLR interaction and endotoxemia (26). In order to determine whether Neu1 contributes to the regulation of *E. coli*-induced TLR4 endocytosis, we established D2SC/1 cell clones stably over-expressing shRNA for Neu1 as described in our recently published work (13, 26), treated these cells with *E. coli* at 37°C for one hour and examined for TLR4 surface levels. As shown in Figure 2A, increased expression of sialylation was observed on the cells over-expressing shRNA for Neu1, compared with the cells expressing scrambled shRNA, however, silencing of Neu1 in D2SC/1 cells has little effect on *E. coli*-induced TLR4 endocytosis (Fig. 2E). In contrast, we made D2SC/1 cell clones stably over-expressing Neu1 and treated these cells with *E. coli* at 37°C for one hour. We found that expression of sialylation was significantly decreased on the cells over-expressing Neu1 compared with empty vector control cells (Fig. 2B) and in our recently published data (13). The efficiency of the *E. coli* induced TLR4 endocytosis was significantly decreased on the cells over-expressing Neu1 compared with cells expressing empty vector, indicating that Neu1 plays an important role in *E. coli*-induced TLR4 endocytosis in D2SC/1 cells (Fig. 2E). Similar results were observed with different stable clones (data not shown).

Glycosyltransferases such as α2-6 sialyltransferase (ST6Gal1) may also modify LacNAc ligands. Therefore, we established D2SC/1 cell clones over-expressing ST6Gal1 (Fig. 2D). Although increased expression of sialylation was observed on the cells over-expressing ST6Gal1 compared with empty vector control cells (Fig. 2C), over-expression of ST6Gal1 in D2SC/1 cells has little effect on *E. coli*-induced TLR4 endocytosis (Fig. 2E). Similar results were observed with different stable clones (data not shown).

Siglec-E is required for *E. coli*-induced TLR4 endocytosis

Siglecs have been shown to be the predominant lectin that binds to sialic acids on cell surface proteins (17), and we have previously found that mouse Siglec-E and F (but not other siglecs) bind strongly to TLR4 (26). Since Siglec-F is mainly expressed on eosinophils (41) and Siglec-E is mainly expressed on dendritic cells, macrophages, and neutrophils (42), here we tested whether Siglec-E is required for *E. coli*-induced TLR4 endocytosis in dendritic cells *in vitro*. We made Siglec-E knockdown cell lines using shRNA specific for Siglec-E. ShRNA silencing of Siglec-E decreases cell surface Siglec-E levels (Fig. 3A), but does not affect the cell surface expression of TLR4 (Fig. 3B). We compared cell surface TLR4 levels in scrambled or Siglec-E shRNA-transduced D2SC/1 cells after treatment with *E. coli* at 37°C for one hour. As shown in Figure. 3C, silencing Siglec-E with lentivirus shRNA reduced *E. coli*-induced TLR4 endocytosis. This coincided with decreased cell surface Siglec-E levels (Fig. 3D) and increased Siglec-E in the cytosol (Fig. 3E). To test if our observed requirement for Siglec-E in *E. coli*-induced TLR4 endocytosis is specific to Siglec-E, we also tested the impact of silencing Siglec-G, which displayed no interaction with any murine TLRs. In contrast to Siglec-E, shRNA silencing of Siglec-G (Fig. 3F) had little effect on *E. coli*-induced TLR4 endocytosis (Fig. 3G). Similar results were observed with different stable clones (data not shown). Next we tested the requirement for Siglec-E in

E. coli-induced TLR4 endocytosis using bone marrow-derived dendritic cells from WT or Siglec-E-deficient mice. Knockout of Siglec-E does not affect the cell surface expression of TLR4 in dendritic cells (Fig. 4A). *E. coli* infection induced endocytosis of TLR4 in WT dendritic cells, but not in cells from Siglec-E-deficient mice (Fig. 4B), and flow cytometric intracellular staining showed increased intracellular TLR4 following *E. coli* infection in WT dendritic cells but not in Siglec-E-deficient dendritic cells (Fig. 4C). As shown in Figure 4D, Siglec-E-deficient dendritic cells produced significantly higher level of TNF-α and IL-6 than WT dendritic cells after infection with *E. coli 25922*. To rule out the possibility that Siglec-E-deficient dendritic cells produced significantly higher level of cytokines was due to the higher load of bacteria in these cells compared with dendritic cells from WT mice, we infected dendritic cells with *E. coli* 25922GFP for one hour and then determined the GFP florescent intensity in these cells by flow cytometry. Bacterial burden in dendritic cells was unaffected in the absence of Siglec-E (Fig. 4E).

To assess the dynamics of Siglec-E contributions to TLR4 internalization, we performed time course analysis for the endocytosis of TLR4. We cultured dendritic cells from WT mice, Siglec-E-deficient mice and CD14-deficient mice. Cell surface TLR4 decreased after a 30- or 60-min infection with *E. coli* on dendritic cells from WT mice, but TLR4 cell surface expression was not reduced on dendritic cells from Siglec-E-deficient mice or CD14-deficient mice (Fig. 4F). Quantification of Mean Fluorescence Intensity shows 50% of the initial TLR4 cell surface expression after 30-min of *E. coli* infection with a further decrease to 35 %-expression after 60 min, on the dendritic cells from WT mice. Less dramatic decreases in cell surface TLR4 were observed with *E. coli* infection on dendritic cells from Siglec-E-deficient mice or CD14-deficient mice (Fig. 4F). Accordingly, the mRNA expression of TNF-α and IL-6 was significantly increased in Siglec-E-deficient dendritic cells compared with the dendritic cells from WT mice or CD14-deficient mice after infection with *E. coli*. TLR4 activates two distinct signaling pathways: the MyD88-dependent and TRIF-dependent pathway. The MyD88-dependent pathway is activated from the plasma membrane after TLR4 encounters LPS. The TRIF-dependent pathway is triggered when TLR4 is delivered to endosomes and mediates the activation of the transcription factor Interferon Regulatory Factor-3 (IRF-3) through dimerization, which regulates Type I interferon (IFN) expression (38, 43). Therefore, we next examined whether LPS-induced expression of Type I interferon and its target genes is altered in the absence of Siglec-E. We found that the mRNA expression of IFN-β and its regulated genes Viperin (38) and MCP-1 (44) were significantly decreased in Siglec-E-deficient dendritic cells infected with *E. coli,* compared with infected dendritic cells from WT mice (Fig. 4G). However, no change in mRNA expression of the Type II interferon, IFN-γ was observed in *E. coli* infected Siglec-E-deficient dendritic cells when compared with WT infected controls (Fig. 4G). It was reported that CD14 controls LPS-induced endocytosis of TLR4 (38), dendritic cells from CD14-deficient mice were used as additional controls. As expected, results from CD14-deficient cells showed decreased IFN-β production with *E. coli* infection (Fig. 4G), consistent with published report (38). Similar results were seen in protein studies. Dendritic cells cultured from Siglec-E-deficient mice and CD14-deficient mice showed significantly decreased secretion of IFN-β in response to *E. coli* treatment, compared with dendritic cells from WT mice (Fig 4H). Accordingly, *E. coli* induced dimerization of IRF3 was not

detected in Siglec-E-deficient dendritic cells (Fig 4I). Collectively, these data suggest that Siglec-E-deficient dendritic cells were defective for TRIF-mediated IFN-β production.

To determine whether our *in vitro* results are relevant to conditions *in vivo*, WT and Siglec-E-deficient mice were treated with PBS or *E. coli* 25922. Since Siglec-E is mainly expressed on dendritic cells, macrophages, and neutrophils (42), we next tested which cell types internalize TLR4 in response to *E. coli* infection. We harvested DCs (CD11c$^+$), macrophages (CD11b$^+$), and B cells (B220$^+$) from the spleen one hour after intravenous (i.v.) injection of *E. coli* 25922 (1×10^6 CFU), and examined TLR4 on the cell surface by flow cytometry. As shown in Figure 5A and B, splenic macrophages and dendritic cells internalized TLR4 in response to *E. coli* infection, and this process was dependent on Siglec-E, CD14 knockout mice were used as controls. The endocytosis of TLR4 was a specific response, as levels of an endocytic receptor (FcγR1, CD64) was largely unaffected by *E. coli* infection (Fig. 5F). In contrast, splenic B cells were not capable of internalizing TLR4 in response to *E. coli* infection (Fig. 5C). Siglec-E-deficient mice produced significantly higher level of TNF-α than WT mice after intravenous injection of *E. coli* 25922 (1×10^6 CFU) for one hour (Fig. 5D). The production of IFN-β was significantly decreased in response to *E. coli* treatment in Siglec-E-deficient mice and CD14-deficient mice, when compared with WT mice (Fig 5E).

Since neutrophils play an important role in the response to bacterial infection and Siglec-E was also expressed on neutrophils, we next tested whether Siglec-E regulates TLR4 internalization in neutrophils. Following infection, cell surface of TLR4 levels were significantly decreased on neutrophils from WT mice, but not from Siglec-E-deficient mice, indicating the Siglec-E plays an important role in the *E. coli*-induced TLR4 endocytosis in neutrophils (Fig. 5G).

Collectively, these data establish that Siglec-E plays a critical role in regulation of *E. coli*-induced TLR4 endocytosis both *in vitro* and *in vivo*. TLR4 endocytosis is Siglec-E-dependent, as it was largely unaffected by knockdown of Siglec-G, and is cell type-specific, as it occurs in macrophages, dendritic cells and neutrophils, but not B cells.

In addition to TLR4, TLR2 was shown to bind to Siglec-E (26). To determine whether Siglec-E also regulates the endocytosis of TLR2 during infection, we examined cell surface expression of TLR2 on dendritic cells, macrophages and neutrophils from WT mice and Siglec-E-deficient mice after infection with *E. coli* 25922 for one hour. The expression of TLR2 on Siglec-E-deficient cell surface was not changed after infection with *E. coli* (Fig. 5H). However, we found that *E. coli* infection induced endocytosis of TLR2 in WT dendritic cells but not in WT macrophage and neutrophils (Fig. 5H). These data suggest that Siglec-E may also play a role in regulation of TLR2 endocytosis in dendritic cells during infection with *E. coli*. The differential role of Siglec-E in TLR2 internalization may be due to the differential sialylation of the TLR2 in these cells, an intriguing possibility for future investigation.

Role of protein kinases in controlling Siglec-E-dependent TLR4 endocytosis

To investigate whether a protein kinase may modulate *E. coli*-induced TLR4 endocytosis, we cultured dendritic cells from Siglec-E-deficient mice and WT littermates, and then treated these cells with *E. coli* in the presence or absence of protein kinase inhibitors. As shown in Figure 6A, inhibition of protein kinase activity of Syk, Src, GSK and ERK efficiently attenuated the *E. coli*-induced TLR4 endocytosis in WT dendritic cells, but inhibition of the protein kinase activity of MEK, ERK, JNK, p38, or PI3K had little effect. Very interestingly, inhibition of the protein kinase activity of PKC promoted endocytosis of TLR4 in Siglec-E-deficient dendritic cells (Fig. 6A). Other inhibitors had little effect on the Siglec-E-deficient cells (Fig. 6A), with the exception of the Syk inhibitor, which efficiently attenuated *E. coli*-induced TLR4 endocytosis (Fig. 6A). In summary, our results indicate that protein kinases Src, GSK and ERK partially contribute to Siglec-E-dependent TLR4 endocytosis. The inhibition activity of Syk inhibitor in *E. coli*-induced TLR4 endocytosis is Siglec-E-independent. PKC inhibitor promoted *E. coli*-induced TLR4 endocytosis in Siglec-E-deficient dendritic cells but not in WT cells, suggesting that Siglec E is a negative regulator of PKC activation during *E. coli* infection.

To test whether the protein kinase inhibitors can affect the production of cytokines, we cultured dendritic cells from Siglec-E-deficient mice and WT littermates, and treated these cells with *E. coli* 25922 in the presence of either the PKC inhibitor GÖ6976 (a specific inhibitor of conventional PKCs, which specifically inhibits PKCα, βI and μ) or the Syk inhibitor piceatannol. As shown in Figure 6B, treatment with *E. coli* resulted in significantly greater production of TNF-α and IL-6 by Siglece $^{-/-}$ dendritic cells than by WT dendritic cells. The observed increase in TNF-α and IL-6 in *E. coli* treated Siglece $^{-/-}$ dendritic cells was abolished in the presence of PKC inhibitor GÖ6976 (Fig. 6B). In contrast, Siglece $^{-/-}$ dendritic cells treated with *E. coli* in the presence of Syk inhibitor piceatannol still produced significantly greater levels of TNF-α and IL-6 when compared with WT dendritic cells (Fig. 6B).

To examine whether PKC inhibitor GÖ6976 can regulate *E. coli*–induced TLR4 endocytosis *in vivo*, WT littermates and Siglec-E-deficient mice were treated with PBS or *E. coli* 25922 in the presence of PKC inhibitor GÖ6976. We harvested dendritic cells (CD11c $^{+}$) from the spleen one hour after intravenous (i.v.) injection of *E. coli* 25922 (1×10^6 CFU) and examined TLR4 surface levels by flow cytometry. As shown in Figure 6C, splenic dendritic cells from Siglec-E-deficient mice are resistant to *E. coli*-induced TLR4 endocytosis, and this resistance was partially rescued by PKC inhibitor GÖ6976, consistent with the data in Figure 6A. In contrast, splenic dendritic cells from WT mice internalized TLR4 in response to *E. coli* infection, and this process was not affected by PKC inhibitor GÖ6976.

The intensity of TLR4-induced phosphorylation of PKC was markedly increased in *E. coli* infected Sigelc-E knockdown D2SC/1 cells (Fig. 7A), bone marrow cultured dendritic cells (Fig. 7B) and splenic CD11c $^{+}$ cells from Siglec-E-deficient mice (Fig. 7C) but not in *E. coli* infected control cells. The intensity of TLR4-induced phosphorylation of p65 was markedly increased in *E. coli* infected Sigelc-E knockdown D2SC/1 cells (Fig. 7A). Moreover, *E. coli* caused greater increases in nuclear translocation of p65 in Siglec-E-deficient dendritic cells than in WT dendritic cells (Fig. 7B). The intensity of TLR4-induced phosphorylation of p38

was markedly increased in *E. coli* infected bone marrow cultured dendritic cells from Siglec-E-deficient mice (Fig. 7B). In contrast, the intensity of TLR4-induced phosphorylation of Erk (Fig. 7A), JNK (Fig. 7A), Src (Fig. 7C), AKT (Fig. 7C), and S6 (Fig. 7 C), is unaffected by loss of Sigelc-E. These data suggest that failure to internalize TLR4 leads to sustained TLR4 surface signaling through activation of NF-κB and MAP kinase p38 in Siglec-E-deficient dendritic cells.

Siglec-E contributes to *E. coli*-induced TLR4 ubiquitination

Endocytosis of plasma membrane-localized TLRs downregulates their signaling functions after a microbial encounter (27, 28). We have here demonstrated that Siglec-E controls *E. coli*-induced TLR4 endocytosis. We next hypothesized that TLR4 may be degraded after endocytosis, and the consequence of the degradation is the termination of signaling during infection. To investigate whether *E. coli* treatment induces TLR4 ubiquitination in dendritic cells, we incubated bone marrow derived-dendritic cells from WT or Siglec-E-deficient mice with *E. coli* at 37°C for one hour. Lysates from these cells were used in immunoprecipitation experiments with anti-TLR4 antibody. The precipitates were probed with anti-ubiquitin antibody and TLR4 antibody. We found that TLR4 ubiquitination was enhanced by *E. coli* treatment in WT dendritic cells, but not in Siglec-E-deficient dendritic cells (Fig. 7D), and the results of co-IP experiment suggests that TLR4 ubiquitination may involve the function of E3 ubiquitin ligase Triad3A (Fig. 7D), which was reported to promote ubiquitin-dependent degradation of TLR4 during infection (45, 46). These data suggest that TLR4 is ubiquitinated as a response to *E. coli* treatment and Siglec-E contributes to *E. coli*-induced TLR4 ubiquitination in dendritic cells.

Siglec-E is required for the resistance of *E. coli*-induced sepsis

We investigated the relevance of our *in vitro* findings with a mouse model of acute septic shock. Siglec-E-deficient mice and WT littermates were challenged with 5×10^5 *E. coli* 25922. The overwhelming majority of the mice with targeted mutation of Siglec-E died within 60 hours, whereas 70% of WT littermates survived the entire period of observation (Fig. 8A). Consistent with the increased mortality of the Siglec-E-deficient mice, the levels of serum TNF-α and IL-6 were substantially higher than the WT littermates controls (Fig. 8B and C). In addition to increased secretion of TNF-α and IL-6, we found that Siglec-E-deficient mice displayed impaired TRIF-mediated IFN-β production (Fig. 8B and C). To rule out the possibility that Siglec-E-deficient mice produced significantly higher level of cytokines was due to the higher load of bacteria compared with WT littermates, we infected WT littermates and Siglec-E-deficient mice with *E. coli* 25922GFP for one hour and then determined the GFP intensity in splenic macrophage, dendritic cells and neutrophils by flow cytometry. Bacterial burden in splenic macrophage, dendritic cells and neutrophils was unaffected in the absence of Siglec-E (Fig. 8D).

Discussion

Sialic acids residues are broadly expressed and potentially act as a marker of self in the immune system (10). Increase in sialylation contributes to the tolerant phenotype in CD4+ T cells (12) and dendritic cells and macrophages (13), while desialylation plays a crucial role

in the recognition process (10) and acts as an "eat me" signal in the clearance of apoptotic cells (15). Here, we found desialylation of cell surface inhibits endocytosis of TLR4 during *E. coli* infection, and our data showed that this is attributable to the action of Neu1 during *E. coli* infection. Expression of Neu1 significantly decreased *E. coli* induced-TLR4 endocytosis, while knockdown of Neu1 has little effect on *E. coli*-induced TLR4 endocytosis.

Siglecs are sialic acid-binding immunoglobin-like lectins. Most Siglecs inhibit immune responses via the recruitment of tyrosine phosphatases such as SHP1 and SHP2 by their cytoplasmic immunoreceptor tyrosine-based inhibitory motifs (ITIM) domain (47). Siglec-E has been shown to play an important role in many immune processes, including binding to the sialylated Tehuantepec strain (48), in negatively regulating of neutrophil recruitment into the lung (49, 50), and in controlling the antiviral response (51). However, it is still unclear whether Siglecs play a role in mediating endocytosis of membrane receptors during infection. We recently reported broad and direct interactions between TLRs and Siglecs, with increased responses from dendritic cells of Siglec-E-deficient mice to all TLR ligands tested (26). Here we further examined the biological significance of this pathway during infection with *E. coli 25922*. We found that Siglec-E is required for *E. coli*-induced TLR4 endocytosis both *in vitro* and *in vivo*. Silencing Siglec-E with lentivirus shRNA in dendritic cell line D2SC/1 cells reduced *E. coli*-induced TLR4 endocytosis, and the TLR4 endocytosis is Siglec-E dependent as it was largely unaffected by knockdown of Siglec-G. The data were further confirmed by using the dendritic cells derived from Siglec-E-deficient mice. We found that the response is cell type-specific, as it occurs in macrophage, neutrophils and dendritic cells, but not B cells. This finding is consistent with the expression pattern of Siglec-E, which is mainly expressed on the macrophage, neutrophils and dendritic cells, but not on B cells (42).

PKC isoforms are important regulators of TLR-mediated innate immune response against pathogens. Recently, PKC was reported to inhibit or promote the process of endocytosis in different kinds of cell types (52–55). Here, we found that *E. coli*-induced endocytosis of TLR4 in Siglec-E-deficient dendritic cells was promoted by inhibition of the protein kinase activity of PKC, but not by other protein kinase inhibitors tested, suggesting that Siglec E is a negative regulator of PKC activation during *E. coli* infection, and PKC is not required for Siglec-E-dependent TLR4 endocytosis. Furthermore, we found that PKC regulates cytokines production after infection with *E. coli* 25922. Treatment with *E. coli* resulted in significantly greater production of TNF-α and IL-6 by Siglece $^{-/-}$ dendritic cells than by WT dendritic cells. This *E. coli* induced increase in TNF-α and IL-6 observed in Siglece $^{-/-}$ cells was completely abolished when in the presence of the PKC inhibitor GÖ6976, but not Syk inhibitor piceatannol. Syk and PKC likely have additional effects on TLR signaling, as we found no clear correlation between the effect of Piceatannol or GÖ6976 on TLR4 endocytosis and cytokine. This is an intriguing area for future investigations.

Ubiquitination is one of the most versatile post-translational modifications of proteins, and plays critical roles in the regulation of innate immune response (56). Recent studies showed that the E3 ubiquitin ligase Triad3A promotes ubiquitin-dependent degradation of TLR4 during infection (45, 46). Interestingly, here we found that ubiquitinated-TLR4 strongly

accumulated in bone marrow derived dendritic cells from WT mice after *E. coli* 25922 infection, but not in bone marrow derived dendritic cells from Siglec-E-deficient mice. Moreover, the binding of E3 ubiquitin ligase Triad3A to TLR4 was significantly increased in bone marrow derived dendritic cells from WT mice after infection, but not in bone marrow derived dendritic cells from Siglec-E-deficient mice, indicating the Siglec-E regulates TLR4 protein levels through altering its state of ubiquitination in dendritic cells.

Siglec-E-deficient dendritic cells showed higher activity of both the MAP kinases p38 and p65 and produced high levels of TNF-α and IL-6 in response to *E. coli* infection, suggesting that failure to internalize TLR4 leads to sustained TLR4 surface signaling through activation of NF-κB and MAP kinase p38. In contrast to the signaling events occurring at the plasma membrane, Siglec-E-deficient dendritic cells produced significantly lower levels of IFN-β in response to *E. coli* infection, indicating that Siglec-E-deficient dendritic cells were also defective for TRIF-mediated IFN-β production. Moreover, the observed higher susceptibility of Siglec-E deficient mice to infection may be due to the increased pro-inflammatory cytokines TNF-α and IL-6 and decreased IFN-β production.

Collectively, these data provides evidence that Siglec-E plays a role in controlling TLR4 endocytosis, and upon entry into the cell, Siglec-E directs TLR4 towards both endosomal signaling and degradation pathways. However, the detailed mechanisms of how Siglec-E controls the two TLR4 signaling pathway are as yet unclear and further investigation is needed to delineate the mechanisms involved.

Acknowledgments

References

1. Hall MJ, Williams SN, DeFrances CJ, Golosinskiy A. Inpatient care for septicemia or sepsis: a challenge for patients and hospitals. NCHS Data Brief. 2011:1–8.

2. Wood KA, Angus DC. Pharmacoeconomic implications of new therapies in sepsis. Pharmacoeconomics. 2004; 22:895–906. [PubMed: 15362927]

3. McClean KL, Sheehan GJ, Harding GK. Intraabdominal infection: a review. Clin Infect Dis. 1994; 19:100–116. [PubMed: 7948510]

4. Bosscha K, Reijnders K, Hulstaert PF, Algra A, van der Werken C. Prognostic scoring systems to predict outcome in peritonitis and intra-abdominal sepsis. Br J Surg. 1997; 84:1532–1534. [PubMed: 9393271]

5. Parrillo JE, Parker MM, Natanson C, Suffredini AF, Danner RL, Cunnion RE, Ognibene FP. Septic shock in humans. Advances in the understanding of pathogenesis, cardiovascular dysfunction, and therapy. Ann Intern Med. 1990; 113:227–242. [PubMed: 2197912]

6. Tracey KJ, Beutler B, Lowry SF, Merryweather J, Wolpe S, Milsark IW, Hariri RJ, Fahey TJ 3rd, Zentella A, Albert JD, et al. Shock and tissue injury induced by recombinant human cachectin. Science. 1986; 234:470–474. [PubMed: 3764421]

7. Moldawer LL. Biology of proinflammatory cytokines and their antagonists. Crit Care Med. 1994; 22:S3–S7. [PubMed: 8026189]

8. Changsirivathanathamrong D, Wang Y, Rajbhandari D, Maghzal GJ, Mak WM, Woolfe C, Duflou J, Gebski V, dos Remedios CG, Celermajer DS, Stocker R. Tryptophan metabolism to kynurenine is a

potential novel contributor to hypotension in human sepsis. Crit Care Med. 2011; 39:2678–2683. [PubMed: 21765346]

9. Rittirsch D, Hoesel LM, Ward PA. The disconnect between animal models of sepsis and human sepsis. Journal of leukocyte biology. 2007; 81:137–143. [PubMed: 17020929]

10. Chen GY, Brown NK, Zheng P, Liu Y. Siglec-G/10 in self-nonself discrimination of innate and adaptive immunity. Glycobiology. 2014; 24:800–806. [PubMed: 24996822]

11. Bi S, Baum LG. Sialic acids in T cell development and function. Biochimica et biophysica acta. 2009; 1790:1599–1610. [PubMed: 19664692]

12. Brennan PJ, Saouaf SJ, Van Dyken S, Marth JD, Li B, Bhandoola A, Greene MI. Sialylation regulates peripheral tolerance in CD4+ T cells. Int Immunol. 2006; 18:627–635. [PubMed: 16291658]

13. Wu Y, Lan C, Ren D, Chen GY. Induction of Siglec-1 by endotoxin tolerance suppresses the innate immune response by promoting TGF-beta1 production. The Journal of biological chemistry. 2016

14. Jenner J, Kerst G, Handgretinger R, Muller I. Increased alpha2,6-sialylation of surface proteins on tolerogenic, immature dendritic cells and regulatory T cells. Exp Hematol. 2006; 34:1212–1218. [PubMed: 16939814]

15. Meesmann HM, Fehr EM, Kierschke S, Herrmann M, Bilyy R, Heyder P, Blank N, Krienke S, Lorenz HM, Schiller M. Decrease of sialic acid residues as an eat-me signal on the surface of apoptotic lymphocytes. Journal of cell science. 2010; 123:3347–3356. [PubMed: 20826457]

16. Crocker PR, Paulson JC, Varki A. Siglecs and their roles in the immune system. Nat Rev Immunol. 2007; 7:255–266. [PubMed: 17380156]

17. Crocker PR. Siglecs: sialic-acid-binding immunoglobulin-like lectins in cell-cell interactions and signalling. Curr Opin Struct Biol. 2002; 12:609–615. [PubMed: 12464312]

18. Yu X, Feizpour A, Ramirez NG, Wu L, Akiyama H, Xu F, Gummuluru S, Reinhard BM. Glycosphingolipid-functionalized nanoparticles recapitulate CD169-dependent HIV-1 uptake and trafficking in dendritic cells. Nat Commun. 2014; 5:4136. [PubMed: 24947940]

19. Tateno H, Li H, Schur MJ, Bovin N, Crocker PR, Wakarchuk WW, Paulson JC. Distinct endocytic mechanisms of CD22 (Siglec-2) and Siglec-F reflect roles in cell signaling and innate immunity. Mol Cell Biol. 2007; 27:5699–5710. [PubMed: 17562860]

20. Jones C, Virji M, Crocker PR. Recognition of sialylated meningococcal lipopolysaccharide by siglecs expressed on myeloid cells leads to enhanced bacterial uptake. Molecular microbiology. 2003; 49:1213–1225. [PubMed: 12940982]

21. Jia Y, Yu H, Fernandes SM, Wei Y, Gonzalez-Gil A, Motari MG, Vajn K, Stevens WW, Peters AT, Bochner BS, Kern RC, Schleimer RP, Schnaar RL. Expression of ligands for Siglec-8 and Siglec-9 in human airways and airway cells. J Allergy Clin Immunol. 2015; 135:799–810. e797. [PubMed: 25747723]

22. von Gunten S, Vogel M, Schaub A, Stadler BM, Miescher S, Crocker PR, Simon HU. Intravenous immunoglobulin preparations contain anti-Siglec-8 autoantibodies. J Allergy Clin Immunol. 2007; 119:1005–1011. [PubMed: 17337295]

23. Bokers S, Urbat A, Daniel C, Amann K, Smith KG, Espeli M, Nitschke L. Siglec-G deficiency leads to more severe collagen-induced arthritis and earlier onset of lupus-like symptoms in MRL/lpr mice. J Immunol. 2014; 192:2994–3002. [PubMed: 24600033]

24. Chen GY, Tang J, Zheng P, Liu Y. CD24 and Siglec-10 selectively repress tissue damage-induced immune responses. Science. 2009; 323:1722–1725. [PubMed: 19264983]

25. Chen GY, Chen X, King S, Cavassani KA, Cheng J, Zheng X, Cao H, Yu H, Qu J, Fang D, Wu W, Bai XF, Liu JQ, Woodiga SA, Chen C, Sun L, Hogaboam CM, Kunkel SL, Zheng P, Liu Y. Amelioration of sepsis by inhibiting sialidase-mediated disruption of the CD24-SiglecG interaction. Nature biotechnology. 2011; 29:428–435.

26. Chen GY, Brown NK, Wu W, Khedri Z, Yu H, Chen X, van de Vlekkert D, D'Azzo A, Zheng P, Liu Y. Broad and direct interaction between TLR and Siglec families of pattern recognition receptors and its regulation by Neu1. eLife. 2014; 3:e04066. [PubMed: 25187624]

27. Husebye H, Halaas O, Stenmark H, Tunheim G, Sandanger O, Bogen B, Brech A, Latz E, Espevik T. Endocytic pathways regulate Toll-like receptor 4 signaling and link innate and adaptive immunity. EMBO J. 2006; 25:683–692. [PubMed: 16467847]

28. Latz E, Visintin A, Lien E, Fitzgerald KA, Espevik T, Golenbock DT. The LPS receptor generates inflammatory signals from the cell surface. J Endotoxin Res. 2003; 9:375–380. [PubMed: 14733724]

29. Biedermann B, Gil D, Bowen DT, Crocker PR. Analysis of the CD33-related siglec family reveals that Siglec-9 is an endocytic receptor expressed on subsets of acute myeloid leukemia cells and absent from normal hematopoietic progenitors. Leuk Res. 2007; 31:211–220. [PubMed: 16828866]

30. Nguyen DH, Ball ED, Varki A. Myeloid precursors and acute myeloid leukemia cells express multiple CD33-related Siglecs. Exp Hematol. 2006; 34:728–735. [PubMed: 16728277]

31. Zhang J, Raper A, Sugita N, Hingorani R, Salio M, Palmowski MJ, Cerundolo V, Crocker PR. Characterization of Siglec-H as a novel endocytic receptor expressed on murine plasmacytoid dendritic cell precursors. Blood. 2006; 107:3600–3608. [PubMed: 16397130]

32. Walter RB, Raden BW, Kamikura DM, Cooper JA, Bernstein ID. Influence of CD33 expression levels and ITIM-dependent internalization on gemtuzumab ozogamicin-induced cytotoxicity. Blood. 2005; 105:1295–1302. [PubMed: 15454492]

33. Avril T, Wagner ER, Willison HJ, Crocker PR. Sialic acid-binding immunoglobulin-like lectin 7 mediates selective recognition of sialylated glycans expressed on Campylobacter jejuni lipooligosaccharides. Infect Immun. 2006; 74:4133–4141. [PubMed: 16790787]

34. Carlin AF, Lewis AL, Varki A, Nizet V. Group B streptococcal capsular sialic acids interact with siglecs (immunoglobulin-like lectins) on human leukocytes. J Bacteriol. 2007; 189:1231–1237. [PubMed: 16997964]

35. Crocker PR. Siglecs in innate immunity. Curr Opin Pharmacol. 2005; 5:431–437. [PubMed: 15955740]

36. Delputte PL, Nauwynck HJ. Porcine arterivirus infection of alveolar macrophages is mediated by sialic acid on the virus. Journal of virology. 2004; 78:8094–8101. [PubMed: 15254181]

37. O'Reilly MK, Tian H, Paulson JC. CD22 is a recycling receptor that can shuttle cargo between the cell surface and endosomal compartments of B cells. J Immunol. 2011; 186:1554–1563. [PubMed: 21178016]

38. Zanoni I, Ostuni R, Marek LR, Barresi S, Barbalat R, Barton GM, Granucci F, Kagan JC. CD14 controls the LPS-induced endocytosis of Toll-like receptor 4. Cell. 2011; 147:868–880. [PubMed: 22078883]

39. Kagan JC, Su T, Horng T, Chow A, Akira S, Medzhitov R. TRAM couples endocytosis of Toll-like receptor 4 to the induction of interferon-beta. Nat Immunol. 2008; 9:361–368. [PubMed: 18297073]

40. Miyagi T, Yamaguchi K. Mammalian sialidases: physiological and pathological roles in cellular functions. Glycobiology. 2012; 22:880–896. [PubMed: 22377912]

41. Macauley MS, Crocker PR, Paulson JC. Siglec-mediated regulation of immune cell function in disease. Nat Rev Immunol. 2014; 14:653–666. [PubMed: 25234143]

42. Zhang JQ, Biedermann B, Nitschke L, Crocker PR. The murine inhibitory receptor mSiglec-E is expressed broadly on cells of the innate immune system whereas mSiglec-F is restricted to eosinophils. European journal of immunology. 2004; 34:1175–1184. [PubMed: 15048729]

43. Rosadini CV, Zanoni I, Odendall C, Green ER, Paczosa MK, Philip NH, Brodsky IE, Mecsas J, Kagan JC. A Single Bacterial Immune Evasion Strategy Dismantles Both MyD88 and TRIF Signaling Pathways Downstream of TLR4. Cell host & microbe. 2015; 18:682–693. [PubMed: 26651944]

44. Yamamoto M, Sato S, Hemmi H, Hoshino K, Kaisho T, Sanjo H, Takeuchi O, Sugiyama M, Okabe M, Takeda K, Akira S. Role of adaptor TRIF in the MyD88-independent toll-like receptor signaling pathway. Science. 2003; 301:640–643. [PubMed: 12855817]

45. Chuang TH, Ulevitch RJ. Triad3A, an E3 ubiquitin-protein ligase regulating Toll-like receptors. Nat Immunol. 2004; 5:495–502. [PubMed: 15107846]

46. Nakhaei P, Mesplede T, Solis M, Sun Q, Zhao T, Yang L, Chuang TH, Ware CF, Lin R, Hiscott J. The E3 ubiquitin ligase Triad3A negatively regulates the RIG-I/MAVS signaling pathway by targeting TRAF3 for degradation. PLoS Pathog. 2009; 5:e1000650. [PubMed: 19893624]

47. Pillai S, Netravali IA, Cariappa A, Mattoo H. Siglecs and immune regulation. Annu Rev Immunol. 2012; 30:357–392. [PubMed: 22224769]

48. Erdmann H, Steeg C, Koch-Nolte F, Fleischer B, Jacobs T. Sialylated ligands on pathogenic Trypanosoma cruzi interact with Siglec-E (sialic acid-binding Ig-like lectin-E). Cellular microbiology. 2009; 11:1600–1611. [PubMed: 19552697]

49. McMillan SJ, Sharma RS, McKenzie EJ, Richards HE, Zhang J, Prescott A, Crocker PR. Siglec-E is a negative regulator of acute pulmonary neutrophil inflammation and suppresses CD11b beta2-integrin-dependent signaling. Blood. 2013; 121:2084–2094. [PubMed: 23315163]

50. McMillan SJ, Sharma RS, Richards HE, Hegde V, Crocker PR. Siglec-E promotes beta2-integrin-dependent NADPH oxidase activation to suppress neutrophil recruitment to the lung. The Journal of biological chemistry. 2014

51. Boyd CR, Orr SJ, Spence S, Burrows JF, Elliott J, Carroll HP, Brennan K, Ni Gabhann J, Coulter WA, Jones C, Crocker PR, Johnston JA, Jefferies CA. Siglec-E is up-regulated and phosphorylated following lipopolysaccharide stimulation in order to limit TLR-driven cytokine production. J Immunol. 2009; 183:7703–7709. [PubMed: 19933851]

52. Cha SK, Wu T, Huang CL. Protein kinase C inhibits caveolae-mediated endocytosis of TRPV5. American journal of physiology. Renal physiology. 2008; 294:F1212–F1221. [PubMed: 18305097]

53. Ferrari SL, Behar V, Chorev M, Rosenblatt M, Bisello A. Endocytosis of ligand-human parathyroid hormone receptor 1 complexes is protein kinase C-dependent and involves beta-arrestin2. Real-time monitoring by fluorescence microscopy. The Journal of biological chemistry. 1999; 274:29968–29975. [PubMed: 10514480]

54. Kanda VA, Purtell K, Abbott GW. Protein kinase C downregulates I(Ks) by stimulating KCNQ1-KCNE1 potassium channel endocytosis. Heart rhythm : the official journal of the Heart Rhythm Society. 2011; 8:1641–1647. [PubMed: 21699843]

55. Linck L, Binder J, Haynl C, Enz R. Endocytosis of GABA(C) receptors depends on subunit composition and is regulated by protein kinase C-zeta and protein phosphatase 1. J Neurochem. 2015; 134:233–246. [PubMed: 25868914]

56. Mohapatra B, Ahmad G, Nadeau S, Zutshi N, An W, Scheffe S, Dong L, Feng D, Goetz B, Arya P, Bailey TA, Palermo N, Borgstahl GE, Natarajan A, Raja SM, Naramura M, Band V, Band H. Protein tyrosine kinase regulation by ubiquitination: critical roles of Cbl-family ubiquitin ligases. Biochimica et biophysica acta. 2013; 1833:122–139. [PubMed: 23085373]

Abbreviations

MAA	fluorescein-Maackia amurensis lectin I, recognizing α2-3–linked terminal sialic acid
MFI	mean fluorescence intensity
PKC	Protein Kinase C
Siglecs	sialic acid-binding Ig (I)-like lectin family members
SNA	fluorescein-Sambucus nigra (elderberry) bark lectin, recognizing α2-6–linked terminal sialic acid
WT	wild-type
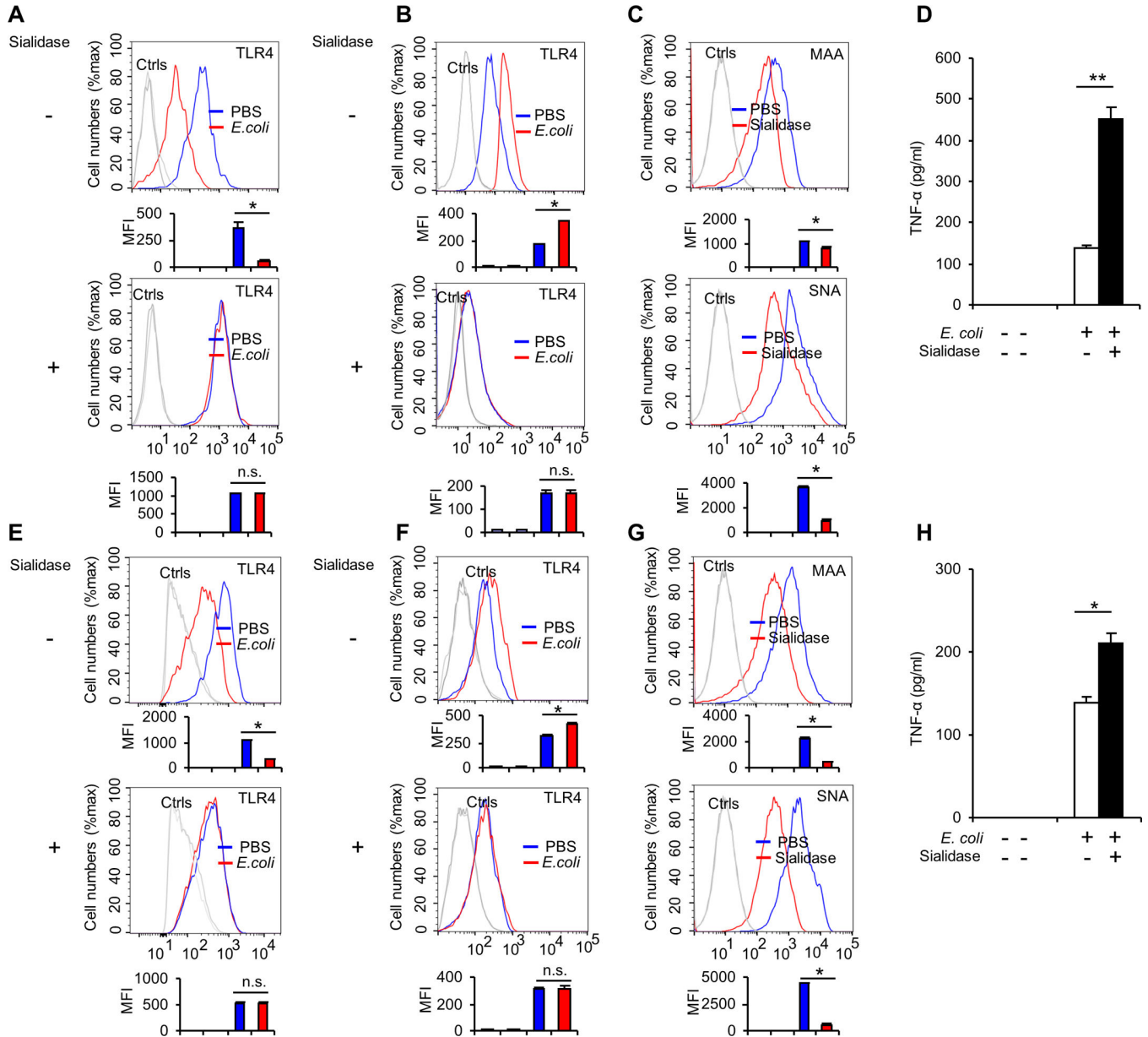
FIGURE 1. The role of sialylation on *E. coli*-induced TLR4 endocytosis

Spleen cells from WT C57BL/6J mouse were first treated with sialidase or PBS at 37°C for one hour and then treated with PBS or *E. coli* 25922 (MOI = 10) at 37°C for one hour. (**A**) Cell surface levels of TLR4 on dendritic cells (gated with CD11c$^+$) were determined by flow cytometry. (**B**) Intracellular staining for TLR4 in dendritic cells (gated with CD11c$^+$). (**C**) Sialidase treatment reduced both α2-3– and α2-6–sialylation of D2SC/1 dendritic cells. Cells were treated as in A, and then stained with MAA or SNA. MAA, fluorescein-Maackia amurensis lectin I, recognizing α2-3–linked terminal sialic acid; SNA, fluorescein-Sambucus nigra (elderberry) bark lectin, recognizing α2-6–linked terminal sialic acid. (**D**) TNF-α in the cell culture supernatants was analyzed with cytokine bead array. Spleen cells from WT C57BL/6J mouse were first treated with sialidase or PBS at 37°C for one hour and

then treated with PBS or *E. coli* 25922 (MOI = 10) at 37°C for five hours. D2SC/1 dendritic cells first were treated with sialidase at 37°C for one hour and then were treated with PBS or *E. coli* 25922 (MOI = 10) at 37°C for one hour. (**E**) Cell surface levels of TLR4 were determined by flow cytometry. (**F**) Intracellular staining for TLR4. (**G**) Sialidase treatment reduced both α2-3– and α2-6–sialylation of D2SC/1 dendritic cells. Cells were stained with MAA or SNA under the same conditions. (**H**) TNF-α in the cell culture supernatants was analyzed with cytokine bead array. D2SC/1 cells were first treated with sialidase or PBS at 37°C for one hour and then treated with PBS or *E. coli* 25922 (MOI = 10) at 37°C for five hours. Representative FACS profiles were shown. The bar graphs under the FACS profiles present the average mean fluorescence intensity (MFI) value ± SEM from one representative experiment (n=3, cells from three different mice in A, B, C and three independent samples in E, F, G), the color on individual bar in the bar graph corresponds to the color of the line in FACS profiles. Experiments depicted in this figure have been reproduced three times.
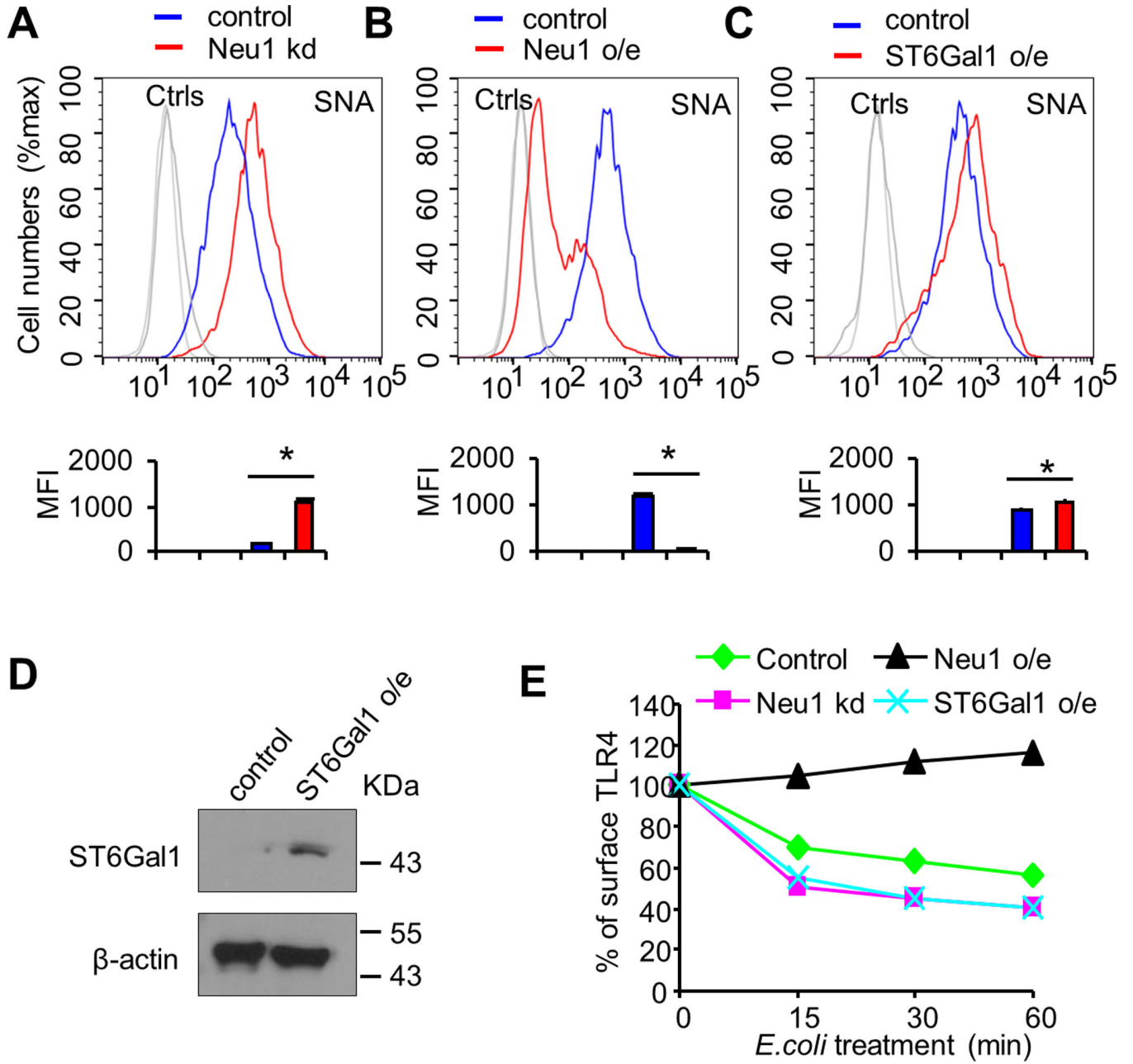
FIGURE 2. A critical role for host Neu1 in *E. coli*-induced TLR4 endocytosis
(**A**) Cell surface of SNA was determined by flow cytometry. D2SC/1 dendritic cells were transduced with lentiviral vector carrying scrambled shRNA or Neu1 shRNA. After transduction and selection with puromycin, stable clones expressing the shRNA were isolated and expanded under the selection of 2 µg/ml puromycin. Neu1 kd, Neu1-knockdown cell line. (**B**) Cell surface of SNA was determined by flow cytometry. D2SC/1 dendritic cells were transfected with vector carrying Neu1 or empty vector as control. Neu1 o/e, stable cell clones over-expressing Neu1. (**C**) Cell surface of SNA was determined by flow cytometry. D2SC/1 dendritic cells were transfected with vector carrying ST6Gal1 or empty vector as control. ST6Gal1 o/e, stable cell clones over-expressing ST6Gal1. (**D**)

Immunobot analysis of ST6Gal1 in D2SC/1 cell clones stably over-expressing vector for Flag-ST6Gal1. Lysates from stable cell clones were subjected to Western blot analysis using anti-Flag antibody. (**E**) Effect of *Neu1* and *ST6Gal1* on *E. coli*-induced TLR4 endocytosis. Indicated D2SC/1 dendritic cell clones were treated with PBS or *E. coli* 25922 (MOI = 10) at 37°C for the indicated time. Flow cytometry was then used to examine TLR4 endocytosis by determining the surface levels of TLR4. Representative FACS profiles were shown in (A), (B) and (C). The bar graphs under the representative FACS profiles present the average MFI value ± SEM from one representative experiment with three independent samples, the color on individual bar in the bar graph corresponds to the color of the line in FACS profiles. Experiments depicted in this figure have been reproduced two times.
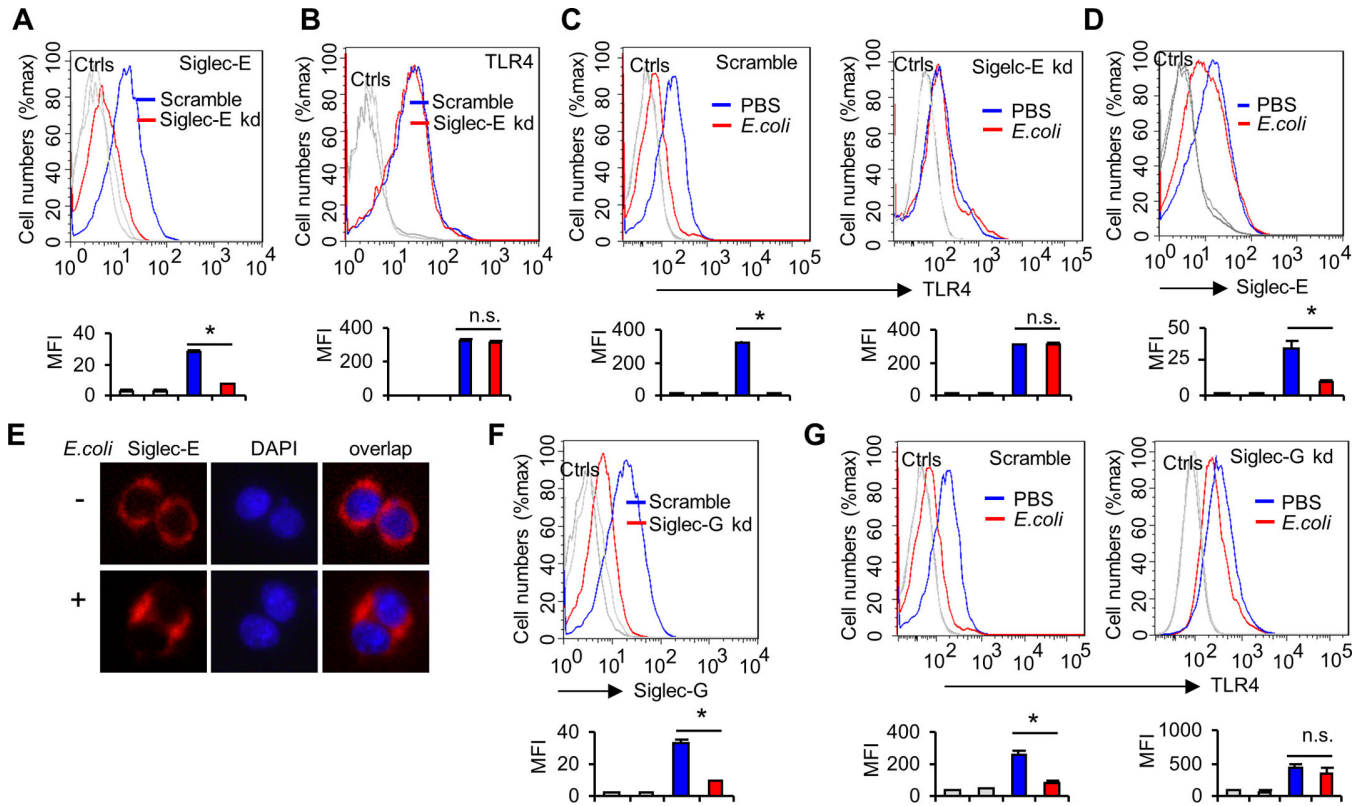
FIGURE 3. Effects of Siglec-E knockdown on *E. coli*-induced TLR4 endocytosis

(**A**) ShRNA silencing of Siglec-E affects cell surface Siglec-E levels. D2SC/1 dentritic cells were transduced with a lentiviral vector carrying scrambled shRNA or Siglec-E shRNA. After transduction and selection with puromycin, stable clones expressing the shRNA were isolated and expanded under the selection of 2 μg/ml puromycin. Data shown are histogram of flow cytometry results depicting cell surface expression of Sigelc-E in D2SC/1 clones. (**B**) Silencing Siglec-E by lentivirus shRNA does not affect the cell surface expression of TLR4. Data shown are histograms of flow cytometry depicting cell surface expression of TLR4 in D2SC/1 clones. (**C**) Silencing Siglec-E by lentivirus shRNA reduces the *E. coli*-induced TLR4 endocytosis. D2SC/1 dendritic cells were treated with PBS or *E. coli* 25922(MOI = 10) at 37°C for one hour. Flow cytometry was then used to examine TLR4 endocytosis by determining the surface levels of TLR4 using anti-TLR4 antibody. (**D**) Expression of Siglec-E on D2SC/1 cell surfaces was determined by flow cytometry. Cells were treated as in c. (**E**) Translocation of Siglec-E in D2SC/1 cells. Cells were plated on chamber slides, treated with PBS or *E. coli* 25922(MOI = 10) at 37°C for one hour and then stained with anti-Siglec-E or DAPI. (**F** and **G**), Siglec-G is not required for *E. coli*-induced TLR4 endocytosis. (**F**) ShRNA silencing of Siglec-G affects cell surface Siglec-G levels. D2SC/1 dendritic cells were transduced with lentiviral vector carrying scrambled shRNA or Siglec-G shRNA. After transduction and selection with puromycin, stable clones expressing the shRNA were isolated and expanded under the selection of 2 μg/ml puromycin. Data shown are histograms of flow cytometry results depicting cell surface expression of Sigelc-G in D2SC/1 clones. (**G**) Silencing Siglec-G by lentivirus shRNA does not affect *E. coli*-induced TLR4 endocytosis. D2SC/1 dendritic cells were treated with PBS or *E. coli*
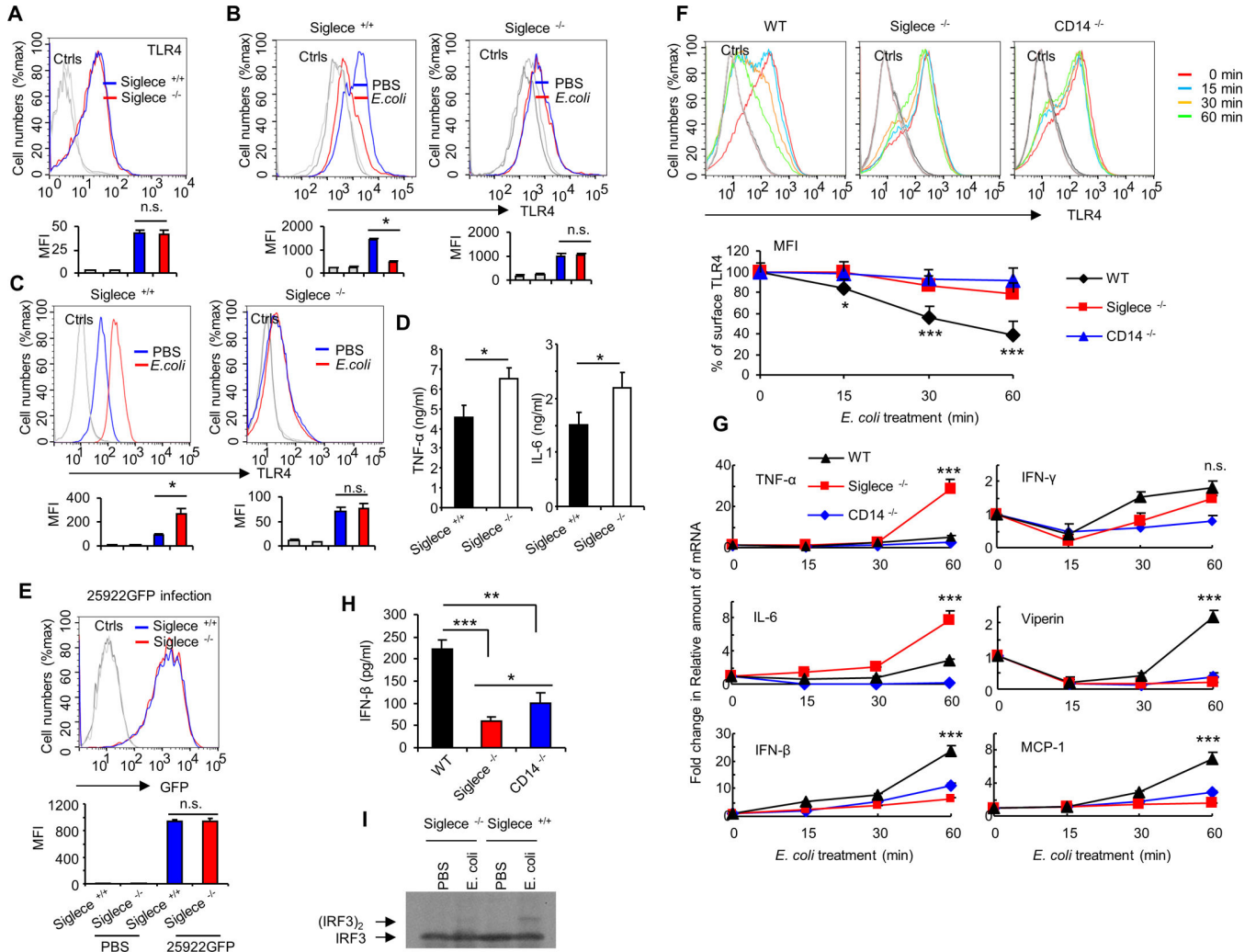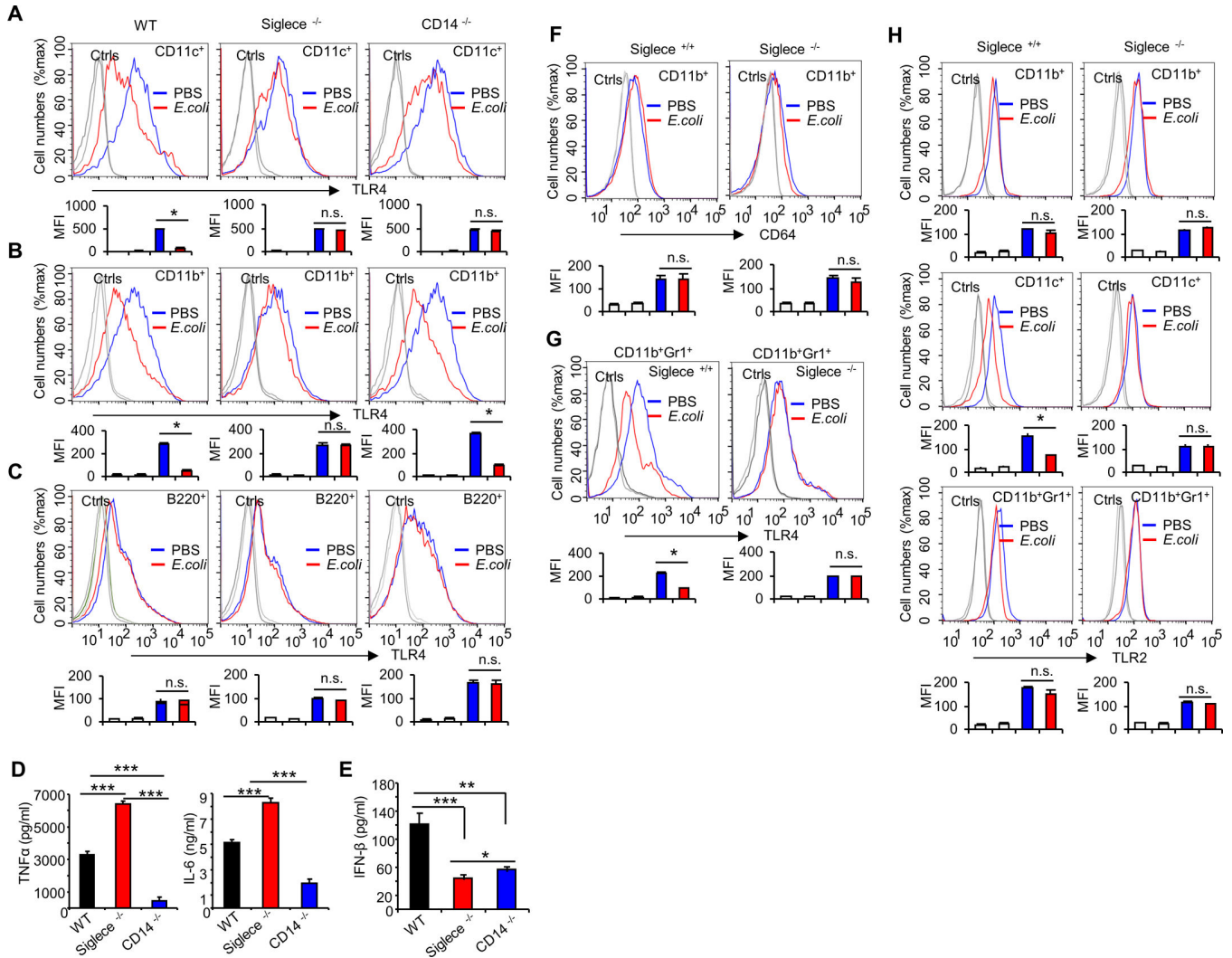
25922(MOI = 10) at 37°C for one hour. Flow cytometry was then used to examine TLR4 endocytosis by determining the cell surface levels of TLR4. Representative FACS profiles were shown. The bar graphs under the representative FACS profiles present the average MFI value ± SEM from one representative experiment with three independent samples, the color on individual bar in the bar graph corresponds to the color of the line in FACS profiles. Experiments depicted in this figure have been reproduced 2–3 times.

FIGURE 4. Siglec-E is required for *E. coli*-induced TLR4 endocytosis *in vitro*
(**A**) Expression of TLR4 on bone marrow derived-dendritic cell surfaces was determined by flow cytometry. Dendritic cells cultured from WT or Siglece $^{-/-}$ bone marrow. (**B**) Bone marrow derived-dendritic cells treated with PBS or *E. coli* 25922 (MOI = 10) at 37°C for one hour. Flow cytometry was then used to examine TLR4 endocytosis by determining the cell surface levels of TLR4. (**C**) Intracellular TLR4 under the same conditions. (**D**) Cytokines in the cell culture supernatants were analyzed with cytokine bead array. Bone marrow derived-dendritic cells were treated with PBS or *E. coli* 25922 (MOI = 10) at 37°C for five hours. (**E**) Bone marrow derived-dendritic cells treated with *E. coli* 25922GFP (MOI = 10) at 37°C for one hour. Flow cytometry was then used to examine GFP fluorescent intensity for detecting the bacterial load in cells. (**F**) WT or Siglec-E-deficient or CD14-deficient mice dendritic cells were untreated or treated with *E. coli* (MOI = 10) for the times indicated. Flow cytometry was then used to examine TLR4 endocytosis by determining the cell surface levels of TLR4. Upper panels show representative profiles, and lower panels show time course as a percentage of initial mean fluorescence intensity. (**G**) Evaluation of the expression of genes in WT or Siglec-E-deficient or CD14- deficient mice dendritic cells untreated or treated with *E. coli* (MOI = 10) for the times indicated by real-time PCR using

specific primer sets. (**H**) IFN-β in the cell culture supernatants were analyzed by ELISA. Bone marrow derived-dendritic cells were treated with PBS or *E. coli* 25922 (MOI = 10) at 37°C for three hours. (**I**) Bone marrow derived-dendritic cells were treated with PBS or *E. coli* 25922 (MOI = 10) at 37°C for one hour and the presence of active (dimerized) IRF3 in the cell extracts was determine by native PAGE. Representative FACS profiles were shown. The bar graphs under the representative FACS profiles present the average MFI value ± SEM from one representative experiment (n = 3, cells from three different mice), the color on individual bar in the bar graph corresponds to the color of the line in FACS profiles. Experiments depicted in this figure have been reproduced 2 or 3 times.

FIGURE 5. Siglec-E is required for *E. coli*-induced TLR4 endocytosis *in vivo*
Splenic cells were collected from WT, Siglece $^{-/-}$ or CD14 $^{-/-}$ mice treated with PBS or *E. coli* 25922 (1×10^6 CFU/mouse, i.v. injection) for one hour. Flow cytometry was then used to examine TLR4 endocytosis by determining the cell surface levels of TLR4 on dendritic cells (CD11c$^+$) (**A**), macrophages (CD11b$^+$) (**B**), or B cells (B220$^+$) (**C**). (**D**) Cytokines and (**E**) IFN-β in the mouse serum were analyzed with cytokine bead array and Elisa, respectively. Serum were isolated from WT or Siglece $^{-/-}$ mice treated with PBS or *E. coli* 25922 (1×10^6 CFU/mouse, i.v. injection) for one hour. (**F**-**H**) Splenic cells were collected from WT or Siglece $^{-/-}$ mice treated with PBS or *E. coli* 25922 (1×10^6 CFU/mouse, i.v. injection) for one hour. Flow cytometry was then used to examine CD64 endocytosis by determining the cell surface levels of CD64 on macrophages (CD11b$^+$) (**F**); Flow cytometry was then used to examine TLR4 endocytosis by determining the cell surface levels of TLR4 on neutrophils (CD11b$^+$Gr1$^+$) (**G**); or Flow cytometry was then used to examine TLR2 endocytosis by determining the cell surface levels of TLR2 on macrophages (CD11b$^+$), on dendritic cells (CD11c$^+$) or neutrophils (CD11b$^+$Gr1$^+$) (**H**). Representative FACS profiles were shown. The bar graphs under the representative FACS profiles present the average MFI value ± SEM

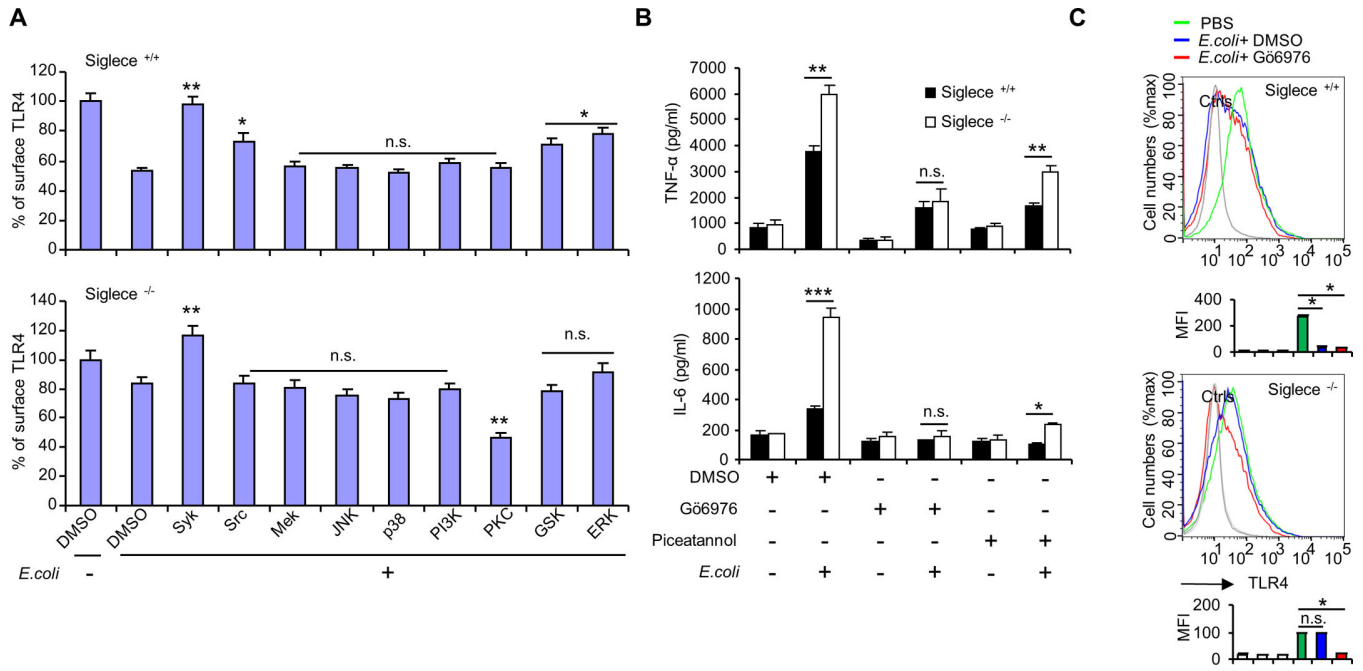from one representative experiment (n = 3, cells from three different mice), the color on individual bar in the bar graph corresponds to the color of the line in FACS profiles. Experiments depicted in this figure have been reproduced 3 times.

FIGURE 6. PKC inhibitor promoted *E. coli*-induced TLR4 endocytosis in Siglec-E-deficient mice and inhibited *E. coli*-induced pro-inflammatory production

(**A**) Dendritic cells cultured from three different WT littermates or Siglece $^{-/-}$ mice were treated with *E. coli 25922* at 37°C for one hour in the presence of indicated protein kinase inhibitors. Flow cytometric analysis was used to determine the cell surface TLR4. Experiments depicted in this figure have been reproduced three times. (**B**) Cytokines in the cell culture supernatant were analyzed with cytokine bead array. Bone marrow-derived dendritic cells from three different mice were treated with *E. coli 25922* in the presence or absence of Syk inhibitor Piceatannol (75 μM) or PKC inhibitor Gö6976 (2.5 μM) at 37°C for 5 hours, and the amount of secreted cytokines were determined. Experiments depicted in this figure have been reproduced two times. (**C**) Five different WT littermates or Siglece $^{-/-}$ mice were pretreated with PKC inhibitor Gö6976 (i.p. injection) for 10 min and then treated with *E. coli 25922* (1×10^6 CFU/mouse, i.v. injection) for one hour. Representative FACS profiles were shown. The bar graphs under the representative FACS profiles present the average MFI value ± SEM from one representative experiment, the color on individual bar in the bar graph corresponds to the color of the line in FACS profiles. Experiments depicted in this figure have been reproduced two times.
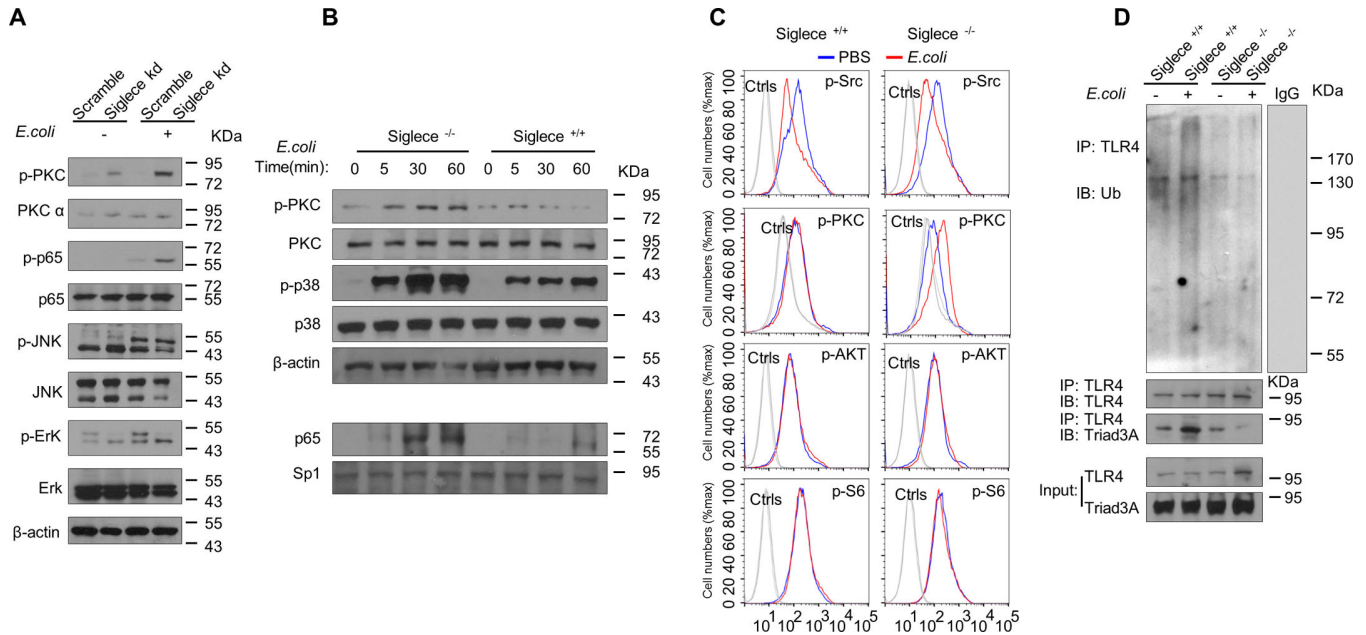
FIGURE 7. Failure to internalize TLR4 leads to activation of NF-κB and MAP kinase p38 and decreased ubiquitination of TLR4 in Siglec-E-deficient dendritic cells

(**A**) Immunoblot analysis of the indicated molecules in lysates of D2SC/1 cell clones stably over-expressing ShRNA for Siglec-E infected with *E. coli* 25922 for one hour. (**B**) Immunoblot analysis of the indicated molecules in lysates from bone marrow derived-dendritic cells from WT littermates or Siglec-E-deficient mice E infected with *E. coli* 25922 for the indicated time. For detecting the activity of NF-κB, the nuclear lysates were prepared and the activation of NF-κB was assessed by blotting for the p65 subunit of NF-κB. The loading of nuclear protein was determined by amount of Sp1 protein. (**C**) Mouse splenic cells were collected after infection with *E. coli* 25922 for one hour, and the expression of p-Src (PBS treated Siglece $^{+/+}$ mice 136.7 ± 9.1 versus *E. coli* treated Siglece $^{+/+}$ mice 114.7 ± 4.2, P <0.05, n=3; PBS treated Siglece $^{-/-}$ mice 125.7 ± 11.6 versus *E. coli* treated Siglece $^{-/-}$ mice 108.3 ± 2.1, P <0.05, n=3), p-PKC (PBS treated Siglece $^{+/+}$ mice 105.7 ± 5.5 versus *E. coli* treated Siglece $^{+/+}$ mice 110.3 ± 10.5, P >0.05, n=3; PBS treated Siglece $^{-/-}$ mice 109.3 ± 4.1 versus *E. coli* treated Siglece $^{-/-}$ mice 141.5 ± 3.6, P <0.05, n=3), p-AKT (PBS treated Siglece $^{+/+}$ mice 67.4 ± 14.8 versus *E. coli* treated Siglece $^{+/+}$ mice 70.7 ± 9.5, P >0.05, n=3; PBS treated Siglece $^{-/-}$ mice 75.3 ± 4.1 versus *E. coli* treated Siglece $^{-/-}$ mice 77.3 ± 6.6, P >0.05, n=3), and p-S6 (PBS treated Siglece $^{+/+}$ mice 194.3 ± 16.9 versus *E. coli* treated Siglece $^{+/+}$ mice 206.7 ± 15.3, P >0.05, n=3; PBS treated Siglece $^{-/-}$ mice 217.3 ± 12.1 versus *E. coli* treated Siglece $^{-/-}$ mice 204.3 ± 7.1, P >0.05, n=3), on dendritic cells (gated with CD11c^{+}) was determined by intracellular staining with corresponding antibodies. Data are mean ± SEM. Experiments depicted in this figure have been produced two times. (**D**) Dendritic cells cultured from WT littermates or Siglece $^{-/-}$ mice were treated with PBS or *E. coli* 25922 (MOI = 10) at 37°C for one hour. TLR4 was immunoprecipitated with a TLR4 antibody and blotted for ubiquitin (FK2 antibody, EMD MILLIPORE), Trad3A and TLR4 antibody. Data representative of outcomes from two independent experiments.
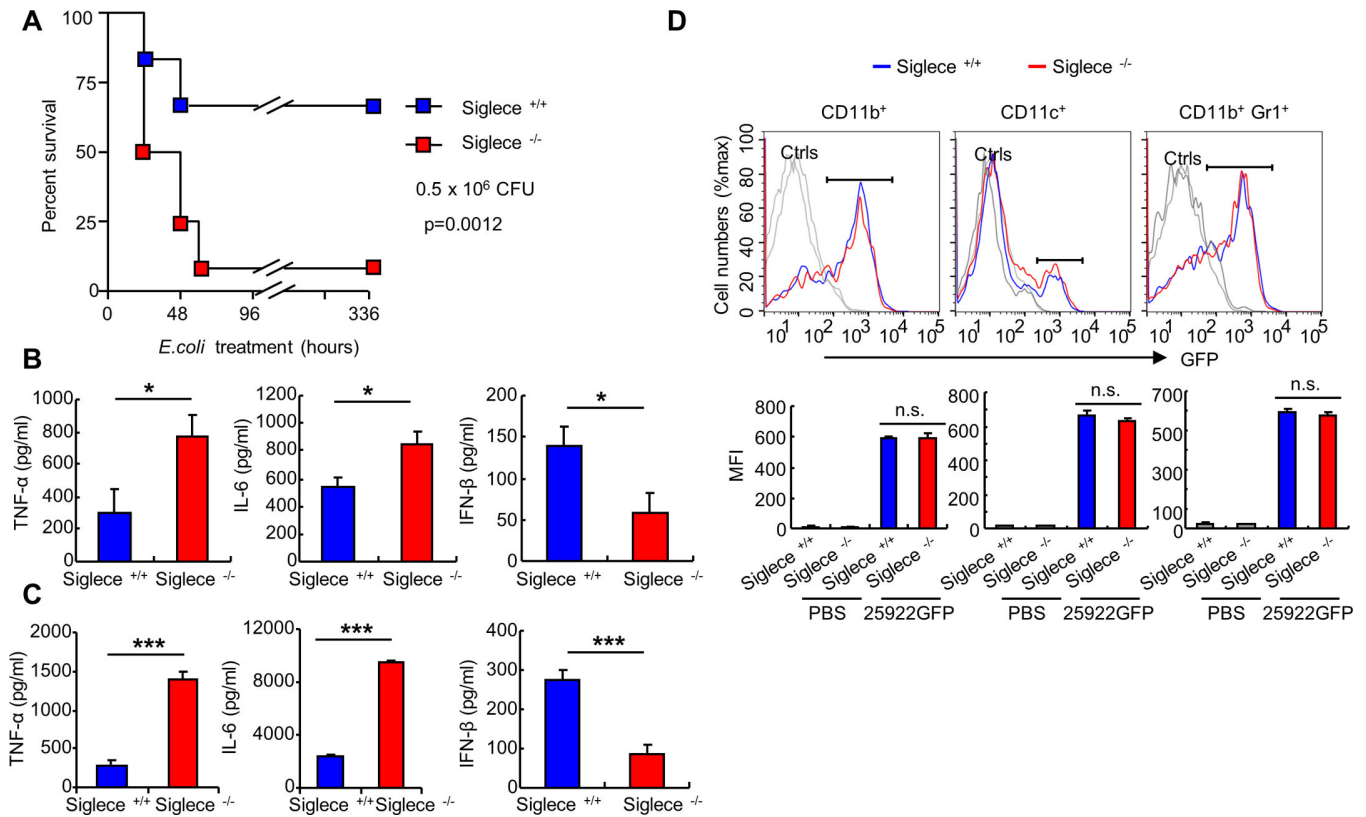
FIGURE 8. Siglec-E deficiency decreases resistance to *E. coli* challenge
(**A**) Survival analyses of Siglece [+/+] and Siglece [−/−] mice that were infected with *E. coli*
25922. The X-axis shows hours after *E. coli* [0.5×10^6 CFU, intraperitoneal (IP) injection]
infection, while the Y-axis shows % of live mice. (n = 8, 6- to 8-week-old male mice were
used). The survival data are presented in the Kaplan Meier survival curve and analyzed by
log-rank tests. (**B**) Serum concentrations of TNF-α, IL-6 and IFN-β at 6 hours after *E. coli*
treatment (mean ± SD, n = 5; *, P < 0.05). (**C**) Serum concentrations of TNF-α, IL-6 and
IFN-β at 20 hours after *E. coli* treatment (mean ± SD, n = 5; ***, P < 0.001). (**D**) Splenic
cells were collected from Siglece [+/+] or Siglece [−/−] mice treated with *E. coli* 25922GFP
(1×10^6 CFU/mouse, i.v. injection) for one hour (n=3, three different mice). Flow cytometry
was then used to examine GFP fluorescent intensity for detecting the bacterial load in
dendritic cells (CD11c^{+}), macrophages (CD11b^{+}), or neutrphils (CD11b^{+}Gr1^{+}).
Representative FACS profiles were shown. The gates used to determine percent positive
cells were labeled in the upper panels. The bar graphs under the FACS profiles present the
average MFI value ± SEM from one representative experiment (n = 3, three different mice),
the color on individual bar in the bar graph corresponds to the color of the line in FACS
profiles. Experiments depicted in this figure have been reproduced two or three times.